The effect of crystallization time on structure, microstructure, and catalytic activity of zeolite-A synthesized from rice husk silica and food-grade aluminum foil

Wasinton Simanjuntak [*], Kamisah D. Pandiangan, Zipora Sembiring, Agustina Simanjuntak, Sutopo Hadi [**]

Department of Chemistry, University of Lampung, Bandar Lampung, Indonesia

ABSTRACT

This study was conducted to evaluate the effect of crystallization time on the structure, microstructure, and catalytic activity of zeolite-A synthesized from rice husk silica and food-grade aluminium foil. Three samples were prepared with fixed crystallization temperature of 100 °C and crystallization times of 48, 72, and 96 h, followed by calcination at 550 °C for 6 h. The samples were characterized using XRD and SEM then used in pyrolysis of mixed solid cassava residue and palm oil. The bio-crude oil (BCO) produced was analyzed using the GC-MS technique. For comparison, a commercial zeolite-A was also characterized and used as the catalyst. Characterization using XRD revealed that zeolite-A has formed at a 48 h crystallization period, with sodalite as a minor component, and crystallization time of 72 h resulted in optimum growth of the zeolite-A. The results of SEM indicated the presence of cubic crystal, most evidently in the sample synthesized with crystallization time of 72 h. This particular sample is the most comparable to a commercial zeolite-A. Pyrolysis experiments produced BCO with hydrocarbons as the main components, with relative percentages of biogasoline fraction (C_6–C_{12}) in the range of 71.88–91.47% in the samples produced using synthesized zeolite and 97.52% using commercial zeolite.

1. Introduction

Efforts to develop renewable energy sources as a response to the depletion of fossil fuel reserves and public awareness of the environmental impacts arising from the use of fossil fuels have placed pyrolysis as one of the biomass to energy conversion methods that continues to attract interest from researchers around the globe. The flexibility in raw material, the simplicity of the technology, short processing time, and the potential of bio-crude oil (BCO) produced to be treated further into higher quality fuel, such as biogasoline, or valuable chemicals are some of the advantages that make pyrolysis a promising technology for sustainable energy supply, liquid fuel in particular. The flexibility of pyrolysis in term of raw material processed is reflected by the application of this thermochemical method to produce BCO from an array of feedstocks such as agricultural wastes [1], mallee wood [2] woody biomass [3], forestry waste [4], oak [5], and pinewood [6].

In practice, pyrolysis of biomass produces gases (low molecular compounds), liquid (consists of water and organics generally known as bio-crude oil), and solid or char. Related to these products, the general finding demonstrates that two main factors showing significant influence on the proportion of each product are raw materials and catalysts, although the role of other factors such as temperature and residence time should also be appreciated. From a renewable energy perspective, BCO is the prime target and in this respect, the optimum formation of this particular product is continuously pursued by exploring different types of catalysts, in an attempt to find the right catalyst for certain raw material. Utilization of the right catalyst is necessary since the experimental results of using different catalysts demonstrated that both the distribution of the product and the composition of the BCO produced are significantly governed by the catalyst used [3]. In search of high-performance catalyst, various types of materials have been developed and tested, with the most widely used are those belong to zeolite materials since this group of the catalyst has been reported to possess reliable deoxygenating activity, resulted in less oxygenated compounds

and richer hydrocarbons in the BCO [1,5,7–11].

Of various synthetic zeolites that have been developed, zeolite-A is known to have varied applications, in which two of the most are as adsorbent and catalyst. As an adsorbent, zeolite-A has been utilized for the removal of several heavy metals from wastewater [12–15]. As the catalyst, this particular zeolite has been utilized for transesterification to convert vegetable oil into biodiesel, which is known as another growing importance renewable liquid fuel [16–18]. These varied utilizations have made zeolite-A an attractive material, drawing continuous interest for exploration of preparation techniques as well as the use of varied raw materials. Some workers have reported the synthesis of zeolite-A from different raw materials, such as sodium metasilicate and by-product from aluminum etching process [19], sodium silicate, and sodium aluminate [20], natural kaolin [21–23], fumed silica and sodium aluminate [24] and rice husk silica [25].

In this current investigation, rice husk silica (RHS) and food-grade aluminum foil were used as raw materials for the synthesis of zeolite-A. While RHS has gained considerable interest as raw material for the production of zeolite, the use of aluminum foil is still very limited, and in this regard, this study was aimed to simultaneously investigate the feasibility of aluminium foil as an alternative precursor of alumina for preparation of synthetic zeolite. The synthesis of zeolite-A was carried out using a hydrothermal process with the main purpose to study the effect of crystallization time on the structure and microstructure of the zeolite resulted. The zeolites produced were then tested as a catalyst for co-pyrolysis of solid cassava residue (SCR) and palm oil, with the general-purpose to evaluate the potential of the zeolites as a catalyst for the production of hydrocarbon-rich BCO, and to compare the chemical composition of BCO produced from utilization of different catalysts.

2. Experimental

2.1. Materials and instruments

Reagent grade sodium hydroxide and nitric acid were purchased from Aldrich. Rice husk (RH) and food-grade aluminum foil (99.9% purity) were purchased from local suppliers in the City of Bandar Lampung. Solid cassava residue (SCR) was obtained from a local cassava processing company, and palm oil was from a local market. Commercial zeolite-A (CAS NO:70955-01-0) was purchased from ACS MATERIAL, Advanced Chemicals Supplier. Polytetrafluoroethylene (PTFE) lined stainless steel autoclave was used for the crystallization process. Calcination was conducted in a Nabertherm electrical furnace (Lilienthal, Germany). PANalytical type Empyrean diffractometer was used for XRD characterization and scanning electron microscope model Zeiss EVO MA 10 was employed for SEM characterization. The pyrolysis experiment was carried out using a laboratory-scale pyrolysis unit, and the BCO produced was analyzed using the GCMS-QP2010 SE SHIMADZU.

2.2. Extraction of RHS

The RHS was obtained using a sol-gel process as reported in the previous study [26]. Typically, a sample of 50 g dried husk was mixed with 500 mL of 1.5% NaOH solution in a beaker glass. The mixture was boiled for 30 min, allowed to cool to room temperature, and then left for 24 h. The mixture was filtered and the filtrate which contains silica (silica sol) was collected. Production of solid silica was carried out by neutralization of the sol using nitric acid 10% to produce a gel, followed by aging of the gel for 24 h, and then repeat rinsing with distilled water to remove the excess of acid, and completed by oven drying of the gel 110 °C for 8 h. Solid RHS was ground into powder and sieved with 250 mesh sieve to obtain the sample with relatively homogeneous sizes. The silica obtained has the purity of 97.86% by XRF analysis.
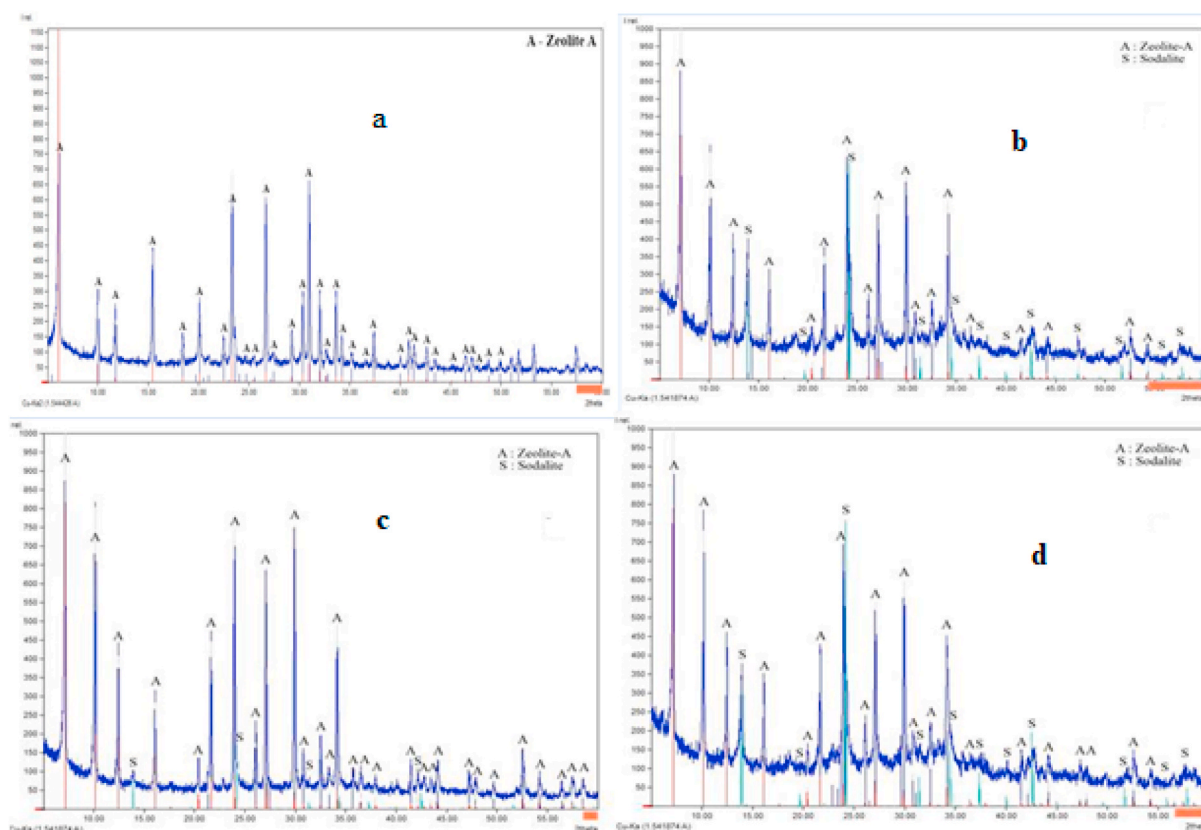

Fig. 1. The XRD patterns of commercial zeolite-A (a) and prepared zeolite-A with different crystallization times: (b) 48 h, (c) 72 h, and (d) 96 h.

Table 1

Comparison of the XRD data for commercial zeolite-A, synthesized zeolite-A, and IZA data. for standard zeolite-A.

IZA Standard		Commercial		This Study					
		Zeolite-A		Zeo-A(48)		Zeo-A(72)		Zeo-A(96)	
$2\,\theta^\circ$	Rel.int. (%)	$2\,\theta^\circ$	Rel.int. (%)	$2\,\theta^\circ$	Rel.int. (%)	$2\,\theta^\circ$	Rel.int. (%)	$2\,\theta^\circ$	Rel.int. (%)
7.194	100.00	6.096_2	100.00	7.193_1	100.00	7.188_6	100.00	7.220_9	100.00
10.181	49.57	9.992_2	25.51	10.177_7	67.35	10.161_6	83.31	10.198_5	74.78
12.477	22.43	11.715_4	19.31	12.475_0	36.86	12.453_1	42.20	12.497_0	37.74
16.129	20.09	15.415_4	41.38	16.119_6	25.83	16.094_0	29.76	16.114_2	26.46
20.443	2.95	20.065_6	21.95	20.433_7	6.15	20.423_2	9.25	20.423_6	8.14
21.698	9.69	20.963_2	3.35	21.652_0	34.49	21.637_1	47.30	21.680_2	37.33

Remark: Zeo-A(48) refers to zeolite-A prepared with a crystallization time of 48 h.
Zeo-A(72) refers to zeolite-A prepared with a crystallization time of 72 h.
Zeo-A(96) refers to zeolite-A prepared with a crystallization time of 96 h.

2.3. Zeolite preparation

Zeolite-A was prepared according to the general formula of (Na_2O. $Al_2O_3 \cdot 2SiO_2 \cdot xH_2O$). A typical sample was prepared by dissolving 40 g NaOH in 350 mL of distilled water, and the solution was divided into two parts. The first part with the volume of 100 mL was used as a solvent to dissolve 27 g of food-grade aluminum foil, and the second portion, with the volume of 250 mL, to dissolve 60 g of RHS. The RHS and aluminum foil solutions were then thoroughly mixed using a laboratory blender, and then the mixture was transferred into a Teflon lined autoclave for 24 h aging process. The autoclave was then placed in an oven set at 100 °C for crystallization times of 48, 72, and 96 h. The solid product was filtered to remove the excess water and then subjected to calcination treatment at 550 °C for 8 h and then ground into powder.

2.4. Zeolite characterization

To investigate whether the zeolite-A was produced as expected, the structure of the samples was evaluated using the X-ray diffraction (XRD) technique and the microstructure using the scanning electron microscopy (SEM) technique. The XRD pattern was produced by PANalytical type Empyrean diffractometer, using CuKα ($\lambda = 1.54$ Å) radiation with the energy of 40 kV and current of 100 mA. The pattern was recorded over the 2 θ range up to 60°, with the scanning rate was $0.06^\circ s^{-1}$. The phase identification was done with the aid of Match! version 3.4.2 Build 96 and confirmed by comparing the XRD-pattern of the sample with that of the standard listed in international zeolite association (IZA) files. The surface morphology of the sample was examined using the SEM technique using Zeiss EVO MA 10 instrument, operated at 30 kV, with an electron acceleration voltage of 20 kV. The sample was scanned at different magnifications for better display of the surface.

2.5. Catalytic activity test

Pyrolysis experiment was performed under an ambient atmosphere in a laboratory scale pyrolysis unit. The reactor is made of stainless steel tube placed inside an iron barrel lined with cement and equipped with a heating element attached to the inside wall of the barrel. The reactor is connected to a power source equipped with temperature control, enabling the pyrolysis to be carried out at a specified temperature. However, the unit is not a temperature programmable, therefore a temperature increase of the pyrolysis process could not be specified. The reactor is connected to a water cooling condenser for the collection of the condensed product. For the pyrolysis experiment, the feedstock (a mixture of 50 g SCR and 150 mL palm oil) was mixed with 10 g of catalyst (zeolite) and then transferred into the pyrolysis unit. The pyrolysis temperature was set at a peak temperature of 400 °C, and pyrolysis was run by heating the reactor until the peak temperature was reached at which the pyrolysis process was allowed to proceed for 60 min. The liquid product was transferred into a separatory funnel and allowed to separate between the water phase and organic phase (BCO). The water layer was drain and the BCO was filtered using Whatman no. 42 filter paper. The chemical composition of the BCO was analyzed using the GC-MS technique equipped with MS Library system NIST12. LIB and WILEY229.LIB.

3. Result and discussion

3.1. Structural study of synthesized zeolites

To examine whether the formation of zeolite-A was achieved with the preparation procedure applied, the commercial zeolite-A and the synthesized samples were characterized with the XRD technique, producing the diffractograms compiled in Fig. 1.

The XRD patterns presented in Fig. 1 show that like commercial zeolite (Fig. 1a), the existence of the samples synthesized as crystalline material is quite evident, as indicated by sharp diffraction peaks in the 2θ range applied (Fig. 1b–d). The diffractograms demonstrated that during the crystallization periods applied, chemical reaction between sodium silicate and sodium aluminate has taken place to a significant extent and led to the formation of crystalline product. Regardless of this crystallite character, the presence of a residual amorphous state should also be acknowledged, which more likely due to unreacted silica and alumina.

To identify the phases present, the diffractogram of each of the samples was analyzed using software Match! Version 3.4.2. With the aid of this software, it was found that the commercial zeolite-A used is a monophasic material. In the samples synthesized, on the other hand, it was found that in addition to zeolite-A as the prominent phase, sodalite was found as a secondary phase. By closer observation of the diffractograms of the samples synthesized (Fig. 1b–d), it can be seen that in general, the diffractograms display a similar appearance, suggesting that during the 48-h crystallization process, the formation of crystalline zeolite-A as the main phase has been achieved and it remains as the main phase in the other two samples. In this respect, the effect of crystallization time is more clearly demonstrated by the presence of sodalite as a secondary phase. As can be seen in the sample with a crystallization time of 48 h, the existence of this secondary phase is indicated by the presence of peaks with noticeable intensity. Extension of crystallization time to 72 h was found to result in the evident reduction of the sodalite phase, as indicated by a significant reduction of the intensity of the peaks associated with this phase. The patterns also display that further extension of crystallization time resulted in increased formation of sodalite phase, as indicated by increased intensity of the peaks associated with this secondary phase. Based on the XRD patterns observed, it is then concluded that the optimum formation of zeolite-A was achieved with a crystallization time of 72 h. Further evaluation was conducted by comparing the XRD data of the commercial zeolite-A and synthesized zeolite-A with those of standard zeolite-A according to IZA. The results are presented in Table 1.
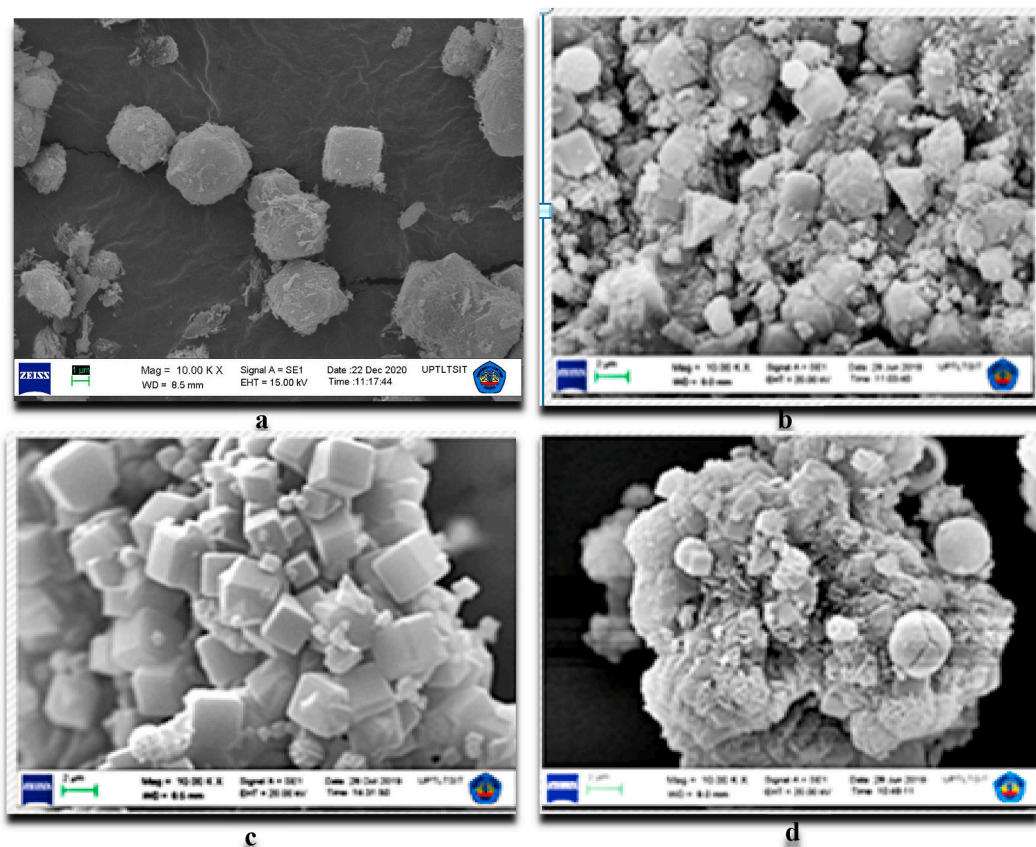
Fig. 2. SEM micrographs of the commercial zeolite-A (a) and the samples prepared with different crystallization times: (b) 48 h, (c) 72 h, and (d) 96 h.

As shown by the data presented in Table 1, six peaks considered as the most prominent peaks characterizing zeolite-A according to IZA standard are found in the samples synthesized. Although the relative intensities of the peaks of the samples are not the same, both between the samples and with those of the IZA standard, except for the first peak, the trend of peak intensity in all samples is similar to that of the IZA standard sample. As can be seen, the intensity of the peak consistently decreases up to the fifth peak and then increases back for the sixth peak. Regarding the XRD features observed, it should also be noted that the zeolites synthesized have a slightly different pattern than that of commercial zeolite-A, which might be due to different raw materials or preparation methods applied.

The agreement between the XRD patterns of the samples and that of IZA standard confirms that zeolite-A has been successfully synthesized, suggesting that aluminum foil can be used as an alternative for more expensive alumina precursors commonly utilized. Concerning the raw materials used, it should be noted that the crystallization time for the optimum formation of zeolite-A was 72 h. Extension of crystallization time to 96 h indicates the transformation of crystalline zeolite-A into sodalite phase, which is in agreement with the finding that zeolite X and zeolite A can be converted into pure sodalite by extending crystallization time or increasing crystallization temperature reported by others [27].

3.2. Microstructural study

In addition to a unique structure as seen by XRD, another distinguishing characteristic of zeolite-A is the cubic structure of its crystal. For this reason, the commercial zeolite-A and the zeolite-A synthesized were characterized using SEM. In addition, to compare the morphology of the samples synthesized to that of the commercial zeolite-A, characterization the samples using SEM is also useful to evaluate the effect of crystallization times on the microstructure of the samples.

The SEM micrographs of the prepared zeolite-A and the commercial zeolite-A are shown in Fig. 2. By comparing the micrographs in Fig. 2, several points are highlighted. The most obvious difference between the commercial and synthesized zeolite-A is that in the micrograph of the commercial zeolite-A, the presence of cubic structure is very obvious and no other structure was observed, confirming its existence as a monophasic material as also indicated by the XRD pattern previously mentioned. For the synthesized samples, on the other hand, the existence of sodalite as a secondary phase is quite evident. In addition, the particles of the commercial zeolite-A are well separated, indicating that they are not agglomerated to form a cluster, while for the synthesized samples agglomeration of the particles is observed. By comparing the micrographs of the samples synthesized it can be seen that the micrograph of the sample prepared with a crystallization time of 72 h is significantly different from those of the other two samples. For this particular sample, the existence of a cubic structure, which is a characteristic shape of crystalline zeolite- A, is very obvious.

This feature is different from the micrographs of the sample prepared with crystallization time of 48 and 96 h, in which the cubic crystals are less evident, and the surface is characterized by the presence of particles with spherical and irregular forms. Based on the XRD results (Fig. 1), it can be inferred that these particles are most likely the sodalite and amorphous RHS that remained unreacted during the crystallization process.

From the surface morphology of the samples, as seen by SEM, it can be inferred that the 48-h crystallization time was not sufficient to optimize the formation of zeolite-A. On the other hand, an extension of crystallization time to 96 h appears to disrupt the zeolite-A structure, leading to the reformation of the sodalite phase. Concerning the results of SEM characterization, the results obtained are in agreement with the results of XRD characterization, in which the two techniques demonstrated that the crystallization process for 72 h resulted in the optimum
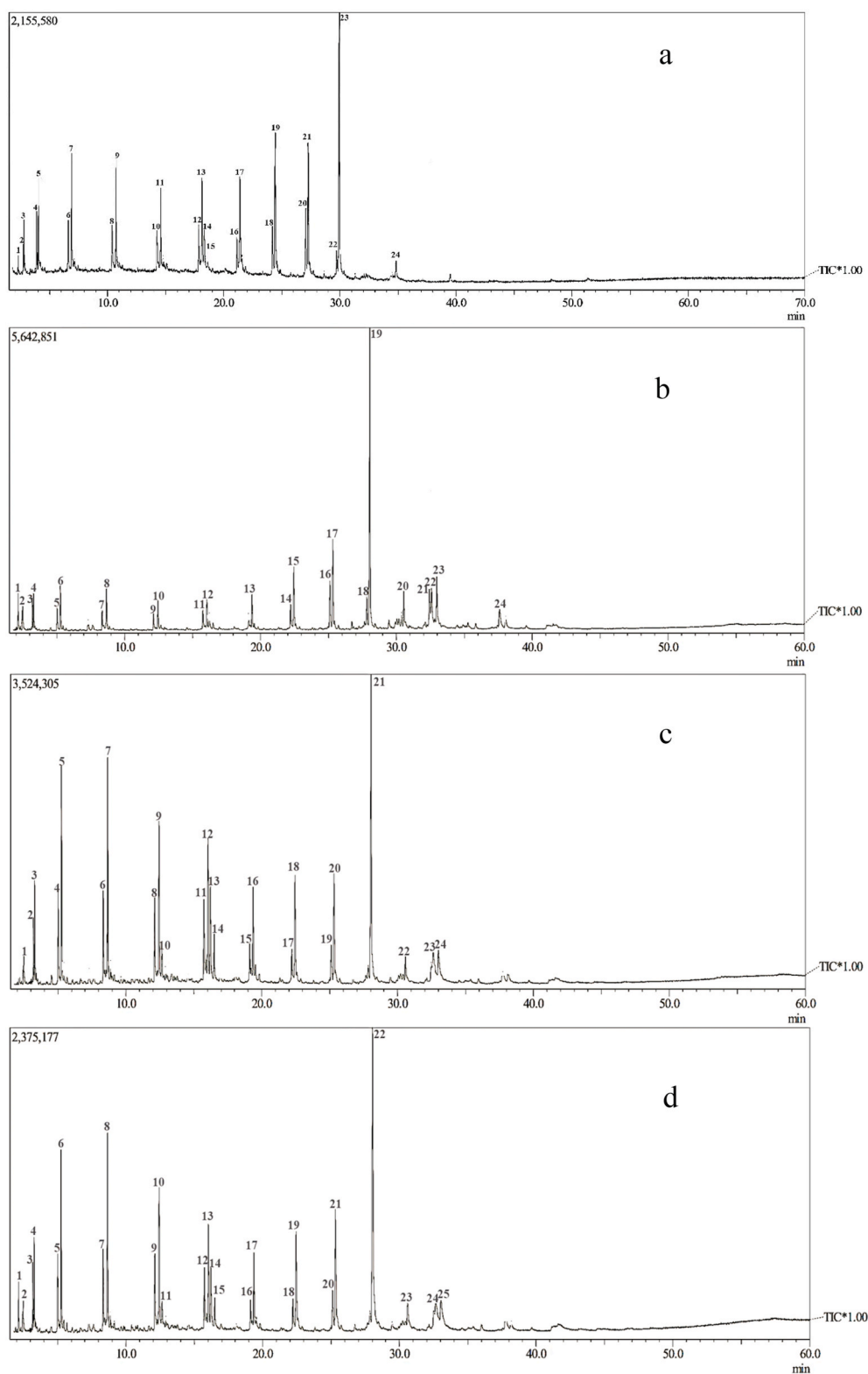
Fig. 3. GC-chromatograms of BCO produced using different catalysts. (a) Commercial zeolite-A, (b) Zeolite-A synthesized with crystallization time of 48 h, (c) Zeolite-A synthesized with crystallization time of 72 h, and (d)) Zeolite-A synthesized with crystallization time of 96 h.

formation of crystalline zeolite-A.

3.3. Catalytic activity test

The GC chromatograms of the BCO produced from the catalytic activity tests carried out using the commercial and synthesized zeolite-A

are shown in Fig. 3. The GC-chromatograms (Fig. 3) display the presence of a series of compounds composing the samples, which is in agreement with a common characteristic of BCO, regardless the types of biomass processed reported by others [28,29]. The chromatograms also indicate a similar trend, in which that the components were eluted in less than 40 min retention time. Also, many of the BCO components were

Table 2
Chemical composition of the BCO produced using different catalysts.

Compound Name	Chemical Formula	Catalyst			
		Zeo-A commercial	Zeo-A (48)	Zeo-A (72)	Zeo-A (96)
Acetone	C_3H_6O	–	1.98	–	1.18
Pentane	C_5H_{12}	0.5	–	–	–
Metil butane	C_5H_{12}	0.81	1.99	1.15	–
Hexane	C_6H_{14}	1.48	–	–	1.37
Heptene	C_7H_{14}	2.28	1.32	1.77	1.61
Heptane	C_7H_{16}	3.19	1.67	2.53	2.44
Octene	C_8H_{16}	2.77	1.58	3.12	2.83
Octane	C_8H_{18}	6.30	3.33	7.31	6.80
Nonene	C_9H_{18}	2.91	1.49	3.37	3.10
Nonane	C_9H_{20}	6.51	3.38	8.31	7.55
Decene isomer	$C_{10}H_{20}$	2.31	1.57	4.22	3.93
Decene isomer	$C_{10}H_{20}$	–	–	6.80	6.16
Decane	$C_{10}H_{22}$	4.77	2.59	1.86	1.76
Undecene isomer	$C_{11}H_{22}$	3.46	1.82	3.98	3.11
Undecane	$C_{11}H_{24}$	5.79	2.49	5.89	4.60
Undecene isomer	$C_{11}H_{22}$	2.92	–	4.27	3.04
Undecene isomer	$C_{11}H_{22}$	1.30	–	1.86	1.28
Undecene isomer	$C_{11}H_{22}$	2.40	–	1.69	1.43
Dodecene isomer	$C_{12}H_{24}$	6.70	2.99	4.31	3.78
Dodecene isomer	$C_{12}H_{24}$	3.58	2.10	1.56	1.78
Dodecene isomer	$C_{12}H_{24}$	8.59	4.99	5.02	5.07
Dodecene isomer	$C_{12}H_{24}$	4.66	4.42	1.92	2.26
Dodecene isomer	$C_{12}H_{24}$	7.71	7.44	5.08	6.26
Dodecene isomer	$C_{12}H_{24}$	1.61	3.01	–	–
Dodecane	$C_{12}H_{26}$	16.28	25.69	16.60	20.04
Tetradecene	$C_{14}H_{28}$	1.17	3.46	–	–
Tetradecane	$C_{14}H_{30}$	–	4.52	–	–
Pentacene	$C_{15}H_{30}$	–	6.20	1.05	1.33
Pentacane	$C_{15}H_{32}$	–	6.46	3.22	3.29
Hexadecane	$C_{16}H_{34}$	–	–	3.15	4.02
2-Heptadecanone	$C_{17}H_{34}O$	–	3.51	–	–

eluted at the same retention times but varied peak intensities, suggesting that the BCO samples are composed of the same chemical components in varying relative amounts. With the aid of the MS Library System NIST12. LIB and WILEY229.LIB, the components of the sample were tentatively identified, while acknowledging that not all of the components were identified, mostly due to very low intensity.

Other Information provided by GC analysis is the relative percentage of each component of the BCO, which can be calculated using the following formula:

$$\%i = \frac{A_i}{A_t} \, x \, 100$$

where: $\%i$ = relative percentage of component i, A_i = peak area of component i, and A_t = total peak area of all identified components.

Since the composition of BCO is generally complex with the presence of a considerably large number of compounds, another way to interpret the data is by allocating each of the components into more general chemical classes. This method is particularly important when comparing several BCO data since practically it is very difficult to compare one sample with the others based on a single component. The identified compounds composing the BCO samples together with other information derived from GC-MS analysis are compiled in Table 2.

The compositional feature of the BCO observed in this study is quite interesting since many researchers involved in biomass pyrolysis have reported significantly more complex compositions of BCO derived from various biomass feedstocks. As an example, the BCO produced by pyrolysis of the wild reed [30] was reported to compose of seven organic categories, namely aliphatic hydrocarbons, acids, oxygenates, phenolics, monocyclic aromatics, polycyclic aromatics, and nitrogen-containing species. Pyrolysis of Napier grass carried out by others [31] was reported to produce BCO with the composition contribute by hydrocarbons, aromatics, phenolics, alcohols, and other oxygenates. In another study [32] the BCO produced from pyrolysis of

raw cellulose was found to consist of aromatics, phenols, furans, and anhydrosugars. In contrast with these previous findings by others which show the presence of oxygen-containing compounds as the dominant contributors to BCO composition, in the present study, as previously mentioned (Table 2), the constituents of the BCO produced are mainly hydrocarbons.

As displayed by the results presented in Table 2, some variations in the components composing the BCO samples are observed, both in terms of the chemical compounds and the relative intensities of the components. The results also indicate that the samples are practically pure hydrocarbons, except the product of using zeo-A(48), in which two ketones were identified. This compositional feature of the BCO produced is under the catalytic nature of zeolites, which is acknowledged to enhance deoxygenation during the pyrolysis of biomass. Also, the hydrocarbons composing the samples in the range of biogasoline (C_6–C_{12}) is quite significant in each of the samples, contributing 71.88–91.47% to the composition of the BCO produced using the synthesized zeolite-A, although these biogasoline contents are lower than that achieved using commercial zeolite-A (97.52%).

4. Conclusion

The experimental results demonstrate that the synthesis of zeolite-A from rice husk silica and food-grade aluminum foil was achieved. Characterization using XRD and SEM reveals that zeolite-A has formed during the 48 h crystallization time, with optimum formation at 72 h crystallization time. Based on XRD and SEM outputs it was found that the structure and microstructure of the zeolite-A synthesized are comparable to those of the commercial zeolite-A, suggesting that RHS and aluminium foil are promising alternative raw materials for the production of zeolite-A. The results of pyrolysis experiments display the very promising performance of zeolite-A synthesized to enhance the production of hydrocarbons and simultaneously reduce the formation of oxygenated compounds in the BCO. Of particular significance is the

zeolite-A synthesized with a crystallization time of 72 h, which was found to produce practically pure hydrocarbon BCO. The biogasoline (C_6–C_{12}) contents of the BCO produced using the synthesized zeolite-A are in the range of 71.88–91.47%.

Acknowledgments

References

[1] E.F. Iliopoulou, K.S. Triantafyllidis, A.A. Lappas, Overview of catalytic upgrading of biomass pyrolysis vapors toward the production of fuels and high-value chemicals, Wiley Interdiscip. Rev. Energy Environ. 8 (2019) 1–29.

[2] H. Wu, D. Gauthier, Y. Yu, X. Gao, G. Flamant, Solar-thermal pyrolysis of mallee wood at high temperatures, Energy Fuels 32 (2018) 4350–4356.

[3] A. Aho, N. Kumar, K. Eranen, B. Holmbom, M. Hupa, T. Salmi, D.Y. Murzin, Pyrolysis of softwood carbohydrates in a fluidized bed reactor, Int. J. Mol. Sci. 9 (2008) 1665–1675.

[4] L. Peng, Y. Wang, Z. Lei, G. Cheng, Co-gasification of wet sewage sludge and forestry waste in situ steam agent, Bioresour. Technol. 114 (2012) 698–702.

[5] M.S.A. Abadi, M. Fathi, M. Ghadiri, Effect of different process parameters on the pyrolysis of iranian oak using a fixed bed reactor and TGA instrument, Energy Fuels 33 (2019) 11226–11234.

[6] X.H. Pham, B. Piriou, S. Salvador, J. Valette, L.V. Steene, Oxidative pyrolysis of pine wood, wheat straw and miscanthus pellets in a fixed bed, Fuel Process. Technol. 178 (2018) 226–235.

[7] L. Zhang, Z. Bao, S. Xia, Q. Lu, K.B. Walters, Catalytic pyrolysis of biomass and polymer wastes, Catalyst 8 (12) (2018) 1–45.

[8] M.U. Garba, U. Musa, A.G. Olugbenga, Y.S. Mohammad, M. Yahaya, A.A. Ibrahim, Catalytic upgrading of bio-oil from bagasse: thermogravimetric analysis and fixed bed pyrolysis, Beni-Suef Univ. J. Basic Appl. Sci. 7 (2018) 776–781.

[9] S.D. Rabiu, M. Auta, A.S. Kovo, An upgraded bio-oil produced from sugarcane bagasse via the use of HZSM-5 zeolite catalyst, Egypt J. Pet. 27 (2018) 589–594.

[10] J.I. Osayi, P. Osifo, Utilization of synthesized zeolite for improved properties of pyrolytic oil derived from used tire, Int. J. Chem. Eng. (2019) 1–12.

[11] S. Tan, Z. Zhang, J. Sun, Q. Wang, Recent progress of catalytic pyrolysis of biomass by HZSM-5, Cuihua Xuebao/Chinese, J. Catal. 34 (2013) 641–650.

[12] Q. Meng, H. Chen, J. Lin, Z. Lin, J. Sun, Zeolite A synthesized from alkaline assisted pre-activated halloysite for efficient heavy metal removal in polluted river water and industrial wastewater, J. Environ. Sci. 56 (2017) 254–262.

[13] C. Wang, J. Li, X. Sun, L. Wang, X. Sun, Evaluation of zeolites synthesized from fly ash as potential adsorbents for wastewater containing heavy metals, J. Environ. Sci. 21 (2009) 127–136.

[14] M. Agarwal Renu, K. Singh, Heavy metal removal from wastewater using various adsorbents: a review, J. Water Reuse. Desalin. 7 (2017) 387–419.

[15] T.S. Jamil, H.S. Ibrahim, I.H.A. El-Maksoud, S.T. El-Wakeel, Application of zeolite prepared from Egyptian kaolin for removal of heavy metals: I. Optimum conditions, Desalination 258 (2010) 34–40.

[16] K.D. Pandiangan, W. Simanjuntak, E. Pratiwi, M. Rilyanti, Characteristics and catalytic activity of zeolite-a synthesized from rice husk silica and aluminium metal by sol-gel method, J. Phys.: Conf. Ser. 1338 (2019) 1–9.

[17] E. Nyankson, J.K. Efavi, A. Yaya, G. Manu, K. Asare, J. Daafuor, R.Y. Abrokwah, M. R. Rashad, Synthesis and characterisation of zeolite-a and Zn-exchanged zeolite-abased on natural aluminosilicates and their potential applications, Cogent. Eng. 5 (2018) 1–23.

[18] V. Volli, M.K. Purkait, Selective preparation of zeolite X and A from flyash and its use as catalyst for biodiesel production, J. Hazard Mater. 297 (2015) 101–111.

[19] K. Hussar, S. Teekasap, N. Somsuk, Synthesis of zeolite A from by-product of aluminum etching process: effects of reaction temperature and reaction time on pore volume, Am. J. Environ. Sci. 7 (2011) 35–42.

[20] Ö. Andaç, M. Tatlier, A. Sirkecioğlu, I. Ece, A.E. Senatalar, Effects of ultrasound on zeolite A synthesis, Microporous Mesoporous Mater. 79 (2005) 225–233.

[21] M. Gougazeh, J.C. Buhl, Synthesis and characterization of zeolite A by hydrothermal transformation of natural Jordanian kaolin, J. Assoc. Arab. Univ. Basic Appl. Sci. 15 (2014) 35–42.

[22] A. Imran, E.A. Bramer, K. Seshan, G. Brem, An overview of catalysts in biomass pyrolysis for production of biofuels, Biofuel. Res. J. 5 (2018) 872–885.

[23] E.B.G. Johnson, S.E. Arshad, Hydrothermally synthesized zeolites based on kaolinite: a review, Appl. Clay Sci. 97 (2014) 215–221.

[24] A.A. Ismail, R.M. Mohamed, I.A. Ibrahim, G. Kini, B. Koopman, Synthesis, Optimization and characterization of zeolite A and its ion-exchange properties, Colloids Surfaces A Physicochem. Eng. Asp. 366 (2010) 80–87.

[25] S.N. Azizi, A.R. Dehnavi, A. Joorabdoozha, Synthesis and characterization of LTA nanozeolite using barley husk silica: mercury removal from standard and real solutions, Mater. Res. Bull. 48 (2013) 1753–1759.

[26] W. Simanjuntak, S. Sembiring, K.D. Pandiangan, F. Syani, R.T.M. Situmeang, The use of liquid smoke as a substitute for nitric acid for extraction of amorphous silica from rice husk through sol-gel route, Orient, J. Chem. 32 (4) (2016) 2079–2085.

[27] M. Tsujiguchi, T. Kobashi, M. Oki, Y. Utsumi, N. Kakimori, A. Nakahira, Synthesis and characterization of zeolite A from crushed particles of aluminoborosilicate glass used in LCD panels, J. Asian Ceram. Soc. 2 (2014) 27–32.

[28] W. Simanjuntak, S. Sembiring, K.D. Pandiangan, E. Pratiwi, F. Syani, Hydrocarbon rich liquid fuel produced by co-pyrolysis of sugarcane bagasse and rubber seed oil using aluminosilicates derived from rice husk silica and aluminum metal as catalyst, Orient, J. Chem. 33 (2017) 3218–3224.

[29] C.A. Mullen, A.A. Boateng, K.B. Hicks, N.M. Goldberg, R.A. Moreau, Analysis and comparison of bio-oil produced by fast pyrolysis from three barley biomass/byproduct streams, Energy Fuels 24 (2010) 699–706.

[30] M.L. Yoo, Y.H. Park, Y.K. Park, S.H. Park, Catalytic pyrolysis of wild reed over a zeolite-based waste catalyst, Energies 9 (2016) 1–9.

[31] I.Y. Mohammed, F.K. Kazi, S. Yusup, P.A. Alaba, Y.M. Sani, Y.A. Abakr, Catalytic intermediate pyrolysis of Napier grass in a fixed bed reactor with ZSM-5, HZSM-5 and zinc-exchanged zeolite-a as the catalyst, Energies 9 (4) (2016) 1–17.

[32] V. Srinivasan, S. Adhikari, S.A. Chattanathan, M. Tu, S. Park, Catalytic pyrolysis of raw and thermally treated cellulose using different acidic zeolites, Bioenergy Res 7 (2014) 867–875.